

# All-Polarization Maintaining Noise-Like Pulse From Mode-Locked Thulium-Doped Fiber Laser Based on Nonlinear Loop Mirror

Yunhong Zhang<sup>ID</sup>, Yi Zheng, Xinyang Su<sup>ID</sup>, Jiying Peng, Haiyang Yu, Tianran Sun, and Huawei Zhang

**Abstract**—In this paper, we present a figure-eight all-polarization maintaining thulium-doped mode-locked fiber laser based on a nonlinear optical loop mirror operating at noise-like pulse regimes. The total cavity length is 34.5 m, and the calculated net group delay dispersion is estimated to be  $\sim -2.616 \text{ ps}^2$ . At the maximum pump power, stable noise-like pulse centered at 1943 nm with a spectral full width at half maximum of 32 nm, a pulse energy of 13.51 nJ, and a coherence spike width of 236 fs is generated at a repetition rate of 5.96 MHz with the signal-to-noise ratio  $\sim 64$  dB. The polarization extinction ratio is  $> 15$  dB at any mode-locking operation. The slope efficiency and the output power fluctuation of the laser are 5.16% and 0.039%, respectively. The laser does not require polarization state controllers, and it holds very high stability, which is insensitive to temperature changes or mechanical vibrations. Through further amplification, it will be a good laser source for real-time interrogation of fiber Bragg gratings and supercontinuum generation.

**Index Terms**—All-polarization maintaining, noise-like pulse, nonlinear optical loop mirror, mode-locked thulium-doped fiber laser.

## I. INTRODUCTION

**T**HULIUM-DOPED fiber laser (TDFL), ranging from 1.7 to 2.1  $\mu\text{m}$ , which is located in the safe band of the human eyes, has a strong water absorption peak, and covers the characteristic spectral lines of many important molecules, owning an important potential application value in space optical communication, biomedicine, precision measurement, material processing [1]. Due to the wide gain spectrum, TDFL is an excellent medium for ultrafast laser pulses. Because of the inherent anomalous dispersion characteristics of silica fiber in 2  $\mu\text{m}$ , conservative soliton is a typical output form of mode-locked thulium-doped silica fiber laser [2]. As we all know, the pulse energy of conservative soliton was restricted to a low level of 0.1 nJ due to the overdriven nonlinear effect [3]. An efficient method to scale the pulse energy in mode-locked fiber lasers is to shift the cavity dispersion from

Manuscript received January 12, 2022; accepted January 16, 2022. Date of publication January 21, 2022; date of current version February 2, 2022. This work was supported in part by the National Natural Science Foundation of China under Grants 61735005 and 61925010, in part by the Natural Science Foundation of Beijing Municipality under Grants 4182054 and 4212052, and in part by the Fundamental Research Funds for the Central Universities under Grant 2021RC206. (*Corresponding author: Yi Zheng.*)

The authors are with the School of Science, Beijing Jiaotong University, Beijing 100044, China (e-mail: 19118047@bjtu.edu.cn; yizheng@bjtu.edu.cn; xysu@bjtu.edu.cn; jypeng@bjtu.edu.cn; yuhaiyang@bjtu.edu.cn; 18118043@bjtu.edu.cn; 18126233@bjtu.edu.cn).

Digital Object Identifier 10.1109/JPHOT.2022.3144413

anomalous to a near-zero dispersion or normal dispersion. In this way, dispersion management soliton [4], dissipative soliton [5], and similariton [6] were demonstrated. In addition, dissipative soliton resonance [7] and noise-like pulse (NLP) were other methods to scale the pulse energy.

NLP is a packet of a large number of ultra-short sub-pulses, with randomly varying amplitudes, durations, and delays between them, furthermore, the pulses are separated by the cavity repetition rate and accompanied with broad smooth spectrum. This kind of pulse can be generated in both normal and anomalous dispersion cavities. It features hundreds of the femtosecond narrow spike atop on the broad pedestal (ps~ns) in autocorrelation trace, this narrow spike is a coherent artifact that arises from the substructure of NLP [8]. Because NLP has low-coherence characteristics, it has great application potential in low-coherence sensing applications, such as real-time interrogation of fiber Bragg gratings [9], real-time monitoring of fiber temperature changes [10], data storage [11]. In addition, high-energy NLP propagates along long fiber segments without distortions, making it particularly suitable for generating supercontinuum [12], [13].

NLP can be generated with different techniques: saturable absorber [14], [15], nonlinear polarization rotation (NPR) [16]–[19], nonlinear optical loop mirrors (NOLM) [20], nonlinear amplifying loop mirror (NALM) [21]–[24], and NOLM in combination with NPR [25]. Mashiko *et al.* utilized chromatic dispersion of telescope lenses and achieved NLP with 1895–1942 nm wavelength tuning range through SESAM [14]. Sobon *et al.* achieved 63 nm spectral full width at half maximum (FWHM) based on a 60-layer graphene/polymer composite [15]. For the technique of NPR, Wang *et al.* reported the first NLP using NPR technique, achieved 15 nm FWHM and 3.1 nJ pulse energy [16]; NLP with 60.2 nm FWHM and 17.3 nJ pulse energy was demonstrated with a piece of thulium-doped germanate glass fiber by He *et al.* [17]; Li *et al.* achieved pretty high pulse energy of 250.1 nJ and FWHM of 18.1 nm [18]. Sobon *et al.* reported an impressive broad emission spectrum (over 300 nm considering 10 dB width) by using a hybrid component (output coupler/isolator/wavelength-division multiplexer) combined with NPR [19]. Li *et al.* achieved pretty high pulse energy of 249.32 nJ and FWHM of 21.33 nm with the technique of NOLM [20]. For the technique of NALM, Zhao *et al.* demonstrated a rectangular NLP with 452 nJ pulse energy located at 1970.3 nm [24]; Michalska *et al.* obtained 32.6 nm FWHM and 11.6 nJ

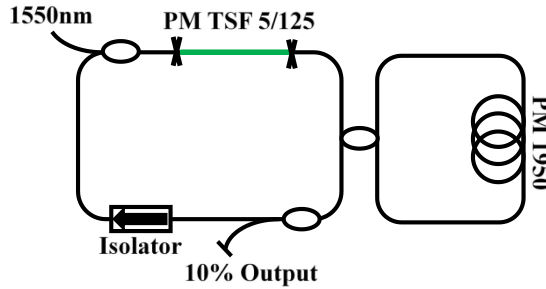


Fig. 1. Experimental setup of all-PM TDFL based on NOLM.

pulse energy by using two pump sources based on NALM [22]; Wang *et al.* achieved  $10 \mu\text{J}$  NLP through three stages amplification [23]. Combining NOLM and NPR, Liu *et al.* demonstrated a single-polarization NLP with  $20 \text{ nm FWHM}$  and  $42.11 \text{ nJ}$  pulse energy [25].

Most of the above mentioned were based on non-polarization maintaining fiber and polarization controller, which tends to be unstable and vulnerable to external disturbances. However, NOLM/ NALM based on polarization-maintaining (PM) fiber is a brilliant solution to resist environmental disturbance. In this paper, we report an all-PM all-fiber TDFL based on NOLM operating at NLP regimes with a broadband spectrum. Compared with the previously reported NLP generation oscillator based on NALM [22], [23], we choose only a piece of short thulium-doped fiber (9.5 cm) as the gain medium and only one pump source, which makes our laser more efficient and economical. In this way, a mode-locked fiber laser with  $32 \text{ nm FWHM}$  and  $13.51 \text{ nJ}$  pulse energy at the fundamental pulse repetition frequency of  $5.96 \text{ MHz}$  is achieved at noise-like pulse regimes. To the best of our knowledge, this is the first demonstration of NLP output from all-PM TDFL based on NOLM.

## II. EXPERIMENTAL SETUP

The experimental setup of the proposed all-PM mode-locked TDFL based on NOLM is shown in Fig. 1. A 9.5 cm long PM Tm-doped fiber (Nufern, PM-TSF-5/125) is used as the gain medium, which has a core diameter of  $5.5 \mu\text{m}$  with a NA of 0.22, and the cladding diameter is  $125 \mu\text{m}$ . The gain fiber is pumped by a 1550 nm CW fiber laser with the maximum output power of 2 W through a 1550/2000 nm PM wavelength-division multiplexer (WDM). The pump source is coupled into the resonant cavity through an FC/APC connector, and the actual power launched into the cavity is 1.884 W. An isolator with an insertion loss of  $0.95 \text{ dB}$  and optical isolation of  $44 \text{ dB}$  at  $2 \mu\text{m}$  is inserted in the ring oscillator to ensure the unidirectional laser operation. A  $2 \times 2$  fused PM coupler centers at 2000 nm with a 20:80 coupling ratio coupled the left loop to the right NOLM. A total of 19 m polarization-maintaining fiber (PM1950, Nufern) is spliced in the nonlinear loop with the aim of decreasing the peak power required to achieve the maximum transmission and ensure enough phase shift difference for stable, self-starting mode-locking. The output of laser pulses is through the 10% port of a 10:90 PM coupler, and it is terminated with an FC/APC type connector.

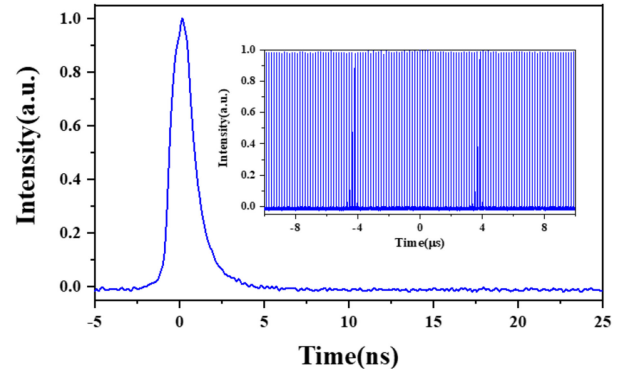


Fig. 2. Pulse train measured by oscilloscope and photodetector, recorded with 5 ns/div and  $2 \mu\text{s}/\text{div}$  (inset).

The length of the total cavity is about 34.5 m including 9.5 cm PM thulium-doped fiber, 19 m PM1950 fiber in the NOLM, and 15.405 m PM1950 pigtail fiber of the couplers and optical isolator. The dispersion of the PM1950 and PM TSF fibers is  $-76 \text{ ps}^2/\text{km}$  and  $-20 \text{ ps}^2/\text{km}$  [26], respectively. The calculated net group delay dispersion (GDD) is estimated to be  $\sim -2.616 \text{ ps}^2$ , suggesting that the laser is operating at a significantly large anomalous dispersion regime. The mode-locked mechanism is based on interference between linear-polarization oscillating light that counter-propagate inside an all-PM fiber loop connected to a laser oscillator via a fiber coupler. An asymmetric splitting ratio of the fiber coupler and a long passive fiber in the loop lead to intensity-dependent loop mirror reflectivity, which can act as a fast modulator of losses in the laser cavity. Therefore, the all-PM-fiber figure-eight laser with NOLM does not require polarization state controllers. It has advantages of less loss, high stability and is insensitive to the environment. In order to achieve efficient heat dissipation from the laser, all the optical fibers are immersed in water and the temperature of the water chiller is set to  $10^\circ\text{C}$ . For the measurements of the laser output, an InGaAs photodetector (EOT ET-5000) with a response time of approximately 28 ps connected to a 3 GHz digital oscilloscope (Lecroy, wavepro 7300A) is used to measure the pulse trains. The spectrum of the laser is measured by a grating spectrometer (Andor, SR-500). A radio-frequency (RF) analyzer (Agilent, N9020A) ranging from 10 Hz to 3.6 GHz is used to study the output pulse sequence in the frequency domain. The pulse duration is measured by an interference autocorrelator (Femtochrome, FR-103XL).

## III. RESULTS AND DISCUSSION

The laser starts to operate at a continuous-wave (CW) regime after reaching the launched pump power of 0.201 W. By continuously increasing pump power, Q-switched mode-locking and multi-pulse state will appear. As the launched pump power increased to 1.005 W, the laser is switched to a stable mode-locked NLP regime without tuning any other elements of the cavity as shown in Fig. 2. At this launched pump power, the average output power is 36.2 mW and the pulse duration is 1.51 ns. The NLP mode-locking state can be maintained until the maximum

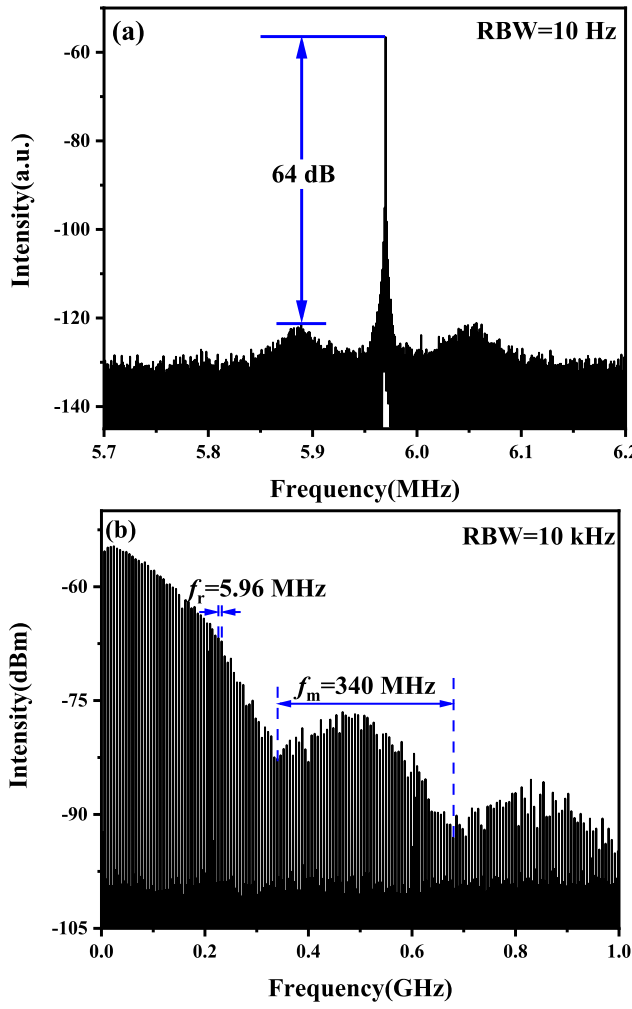


Fig. 3. RF spectrums with a scanning range of (a) 0.5 MHz and (b) 1 GHz.

pump power without pulse breaking or multi-pulse operation. The average output power is 80.5 mW with the maximum pump power of 1.884 W. The polarization extinction ratio (PER) of the laser is  $>15$  dB at any mode-locking operation measured by an ultra-broadband wire grid linear polarizer (Edmund, 34-315) with an extinction ratio of 5000:1.

A radio frequency (RF) spectrum around the fundamental repetition rate of 5.96 MHz by using 10-Hz resolution bandwidth (RBW) is described in Fig. 3(a), showing a signal-to-noise ratio (SNR)  $\sim 64$  dB, which is better than reported previously [13], [21]. There are two broad symmetrical spectral sidebands around the fundamental repetition rate, which reveals the existence of random peak modulation of the mode-locked pulses. This noise pedestal is typical for NLP lasers. This proves that the pulse is NLP [27], [28]. Fig. 3(b) shows the corresponding RF spectral distribution with 1 GHz span by using 10 kHz RBW. Both Fig. 3(a) and (b) are recorded with 1.884 W pump power. Once the mode-locked state is achieved, a series of smooth broad-spectrum is observed as shown in Fig. 4(b). As the pump power increases, the spectral intensity increases and the bandwidth becomes broader, but the central wavelength remains around 1943 nm. When the pump power is 1.884 W, the maximum FWHM of 32 nm at the central wavelength of 1943 nm is

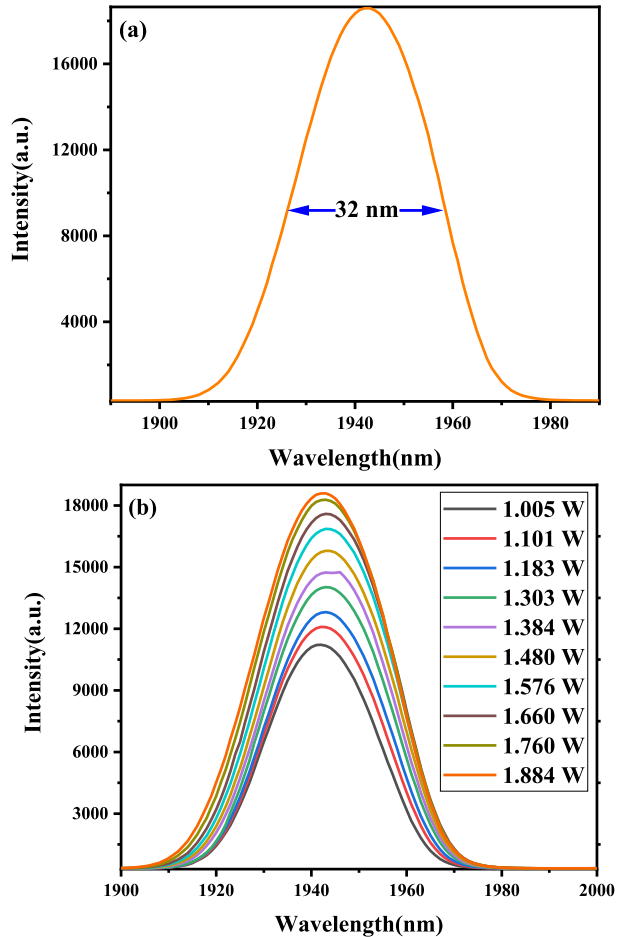


Fig. 4. Output spectrum (a) at the maximum pump of 1.884 W and (b) at different pump powers.

obtained, which is shown in Fig. 3(a). However, at the maximum pump power, the corresponding autocorrelation trace cannot be measured due to the small average power. By amplifying the power to 111 mW, the autocorrelation trace is observed (as shown in Fig. 5(a)). The autocorrelation trace shows a narrow spike riding on a broad, which is a classic signature of the NLP. The autocorrelation trace shown is not symmetric and smooth, which may attribute to the mirror inside the autocorrelator. It is partly damaged and has a poor reflection. But this has a very weak impact on the final results we obtain. Fig. 5(b) shows the autocorrelation trace as the scanning range further reduces to 3 ps. Assuming a Gaussian-pulse profile, the measured curve is fitted with a coherence spike width of 236 fs. In addition, the shoulder to peak exhibits a 1:1.46 ratio instead of typical 1:8 for the solitary mode-locking, suggesting that there is a bunch of pulses with varying width and power overlapped in a large time scale [16].

The average output power, pulse energy, and pulse duration as a function of the launched pump power is shown in Fig. 6(a) and (b). It can be seen that the average power, pulse energy, and pulse duration increase linearly as the pump power increases. For a stable mode-locking state, a slope efficiency of 5.16% is observed. With the maximum launched pump power of 1.884 W, the maximum average output power of 80.5 mW is obtained,

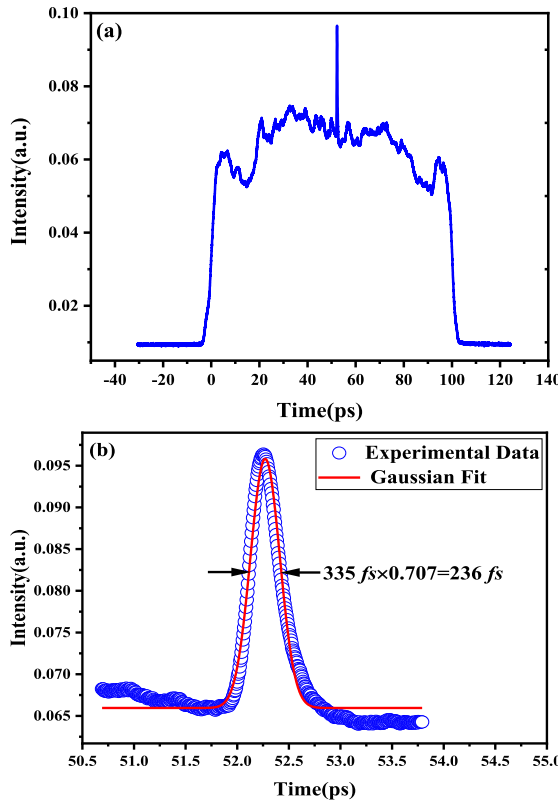


Fig. 5. The autocorrelation trace of NLP with scanning range of (a) 150 ps and (b) 3 ps with Gaussian fit.

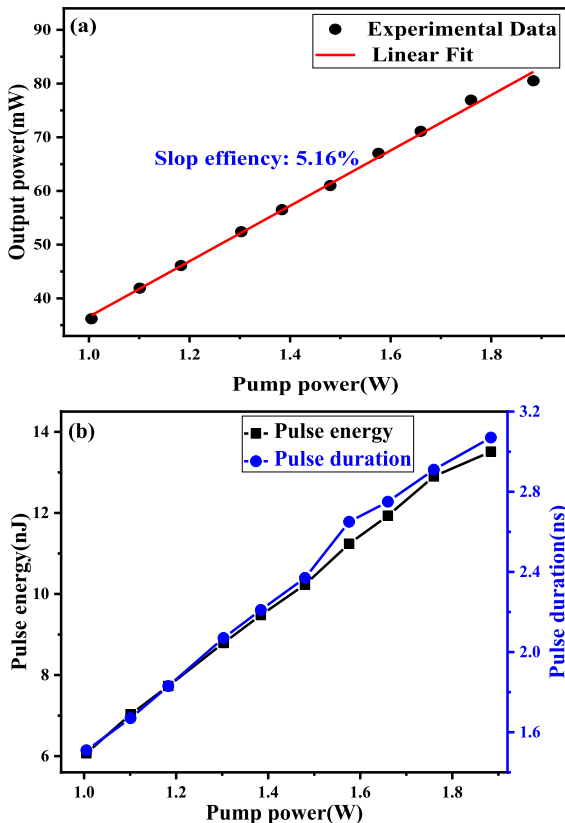


Fig. 6. (a) Output power versus the pump power, (b) NLP energy (black) and duration (blue) versus the pump power.

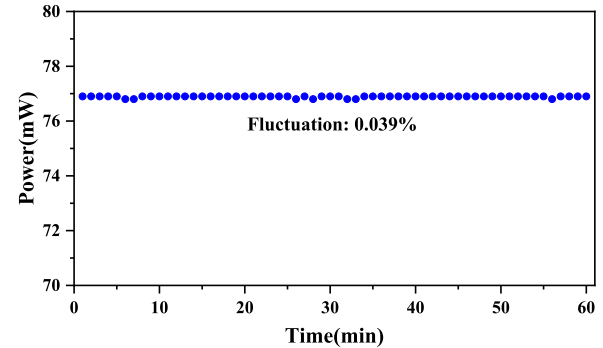


Fig. 7. The average output power fluctuation of the NLP within 1h.

corresponding to the pulse energy of 13.51 nJ. To evaluate the stability of the mode-locked laser, the average output power of the NLP operation is monitored every minute within one hour as shown in Fig. 7. The fluctuation is 0.039% in one hour's measurement, and 0.074% for two hours' measurement. We think the reason for the slight power fluctuation is as follows, the water cooling does not take away the heat in time at the end of another working cycle, which causes the ambient temperature to rise, leading to a slight decrease in average output power. If we use a water chiller with better temperature control, a more stable output may be achieved.

#### IV. CONCLUSION

In summary, we have first experimentally demonstrated a figure-eight all-PM TDFL mode-locked with a NOLM operating at NLP regimes. When the launched pump power is 1.884 W, a 5.96 MHz, 13.51 nJ, NLP centered at 1943 nm is obtained, with the coherence spike width of 236 fs. The NLP output with the coefficient of variation of 0.039%. Through further amplification, it will be a good laser source for real-time interrogation of fiber Bragg gratings and supercontinuum generation.

#### REFERENCES

- [1] J. Ma, Z. Qin, G. Xie, L. Qian, and D. Tang, "Review of mid-infrared mode-locked laser sources in the 2.0  $\mu\text{m}$ -3.5  $\mu\text{m}$ , spectral region," *Appl. Phys. Rev.*, vol. 6, no. 2, Jun. 2019, Art. no. 021317.
- [2] D. Zhao *et al.*, "Improvements of soliton pulse energy and peak power in thulium-doped fiber laser," *IEEE Photon. Technol. Lett.*, vol. 31, no. 11, pp. 909–912, Jun. 2019.
- [3] H. A. Haus, K. Tamura, L. E. Nelson, and E. P. Ippen, "Stretched-pulse additive-pulse mode-locking in fiber ring lasers - Theory and experiment," *IEEE J. Quantum Electron.*, vol. 31, no. 3, pp. 591–598, Mar. 1995.
- [4] F. Haxsen, A. Ruehl, M. Engelbrecht, D. Wandt, U. Morgner, and D. Kracht, "Stretched-pulse operation of a thulium-doped fiber laser," *Opt. Exp.*, vol. 16, no. 25, pp. 20471–20476, Dec. 2008.
- [5] N. Yang, C. Huang, Y. Tang, and J. Xu, "12 Nj 2  $\mu\text{m}$  dissipative soliton fiber laser," *Laser Phys. Lett.*, vol. 12, no. 5, Mar. 2015, Art. no. 055101.
- [6] Y. Tang, A. Chong, and F. W. Wise, "Generation of 8 Nj pulses from a normal-dispersion thulium fiber laser," *Opt. Lett.*, vol. 40, no. 10, pp. 2361–2364, May 2015.
- [7] Z. Zheng, D. Ouyang, X. Ren, J. Wang, J. Pei, and S. Ruan, "033 MJ, 1043 W dissipative soliton resonance based on a figure-of-9 double-clad Tm-doped oscillator and an all-fiber mopa system," *Photon. Res.*, vol. 7, no. 5, May 2019, Art. no. 000513.

- [8] A. F. J. Runge, C. Aguergaray, N. G. R. Broderick, and M. Erkintalo, "Coherence and shot-to-shot spectral fluctuations in noise-like ultrafast fiber lasers," *Opt. Lett.*, vol. 38, no. 21, pp. 4327–4330, Nov. 2013.
- [9] S. Keren and J. Moshe, "Interrogation of fiber gratings by use of low-coherence spectral interferometry of noiselike pulses," *Opt. Lett.*, vol. 26, no. 6, pp. 328–330, 2001.
- [10] V. Goloborodko, S. Keren, A. Rosenthal, B. Levit, and M. Horowitz, "Measuring temperature profiles in high-power optical fiber components," *Appl. Opt.*, vol. 42, no. 13, pp. 2284–2288, May 2003.
- [11] S. Keren, E. Brand, Y. Levi, B. Levit, and M. Horowitz, "Data storage in optical fibers and reconstruction by use of low-coherence spectral interferometry," *Opt. Lett.*, vol. 27, no. 2, pp. 125–127, Jan. 2002.
- [12] A. Camarillo-Avilés, R. López-Estopier, O. Pottiez, M. Durán-Sánchez, B. Ibarra-Escamilla, and M. Bello-Jiménez, "Supercontinuum source directly from noise-like pulse emission in a Tm-doped all-fiber laser with nonlinear polarization rotation," *Results Opt.*, vol. 2, Dec. 2021, Art. no. 100040.
- [13] H. Ahmad, M. H. M. Ahmed, and M. Z. Samion, "Generation of mode-locked noise-like pulses in double-clad Tm-doped fibre laser with nonlinear optical loop mirror," *J. Mod. Opt.*, vol. 67, no. 2, pp. 146–152, Jan. 2020.
- [14] Y. Mashiko, E. Fujita, and M. Tokurakawa, "Tunable noise-like pulse generation in mode-locked tm fiber laser with a sesam," *Opt. Exp.*, vol. 24, no. 23, pp. 26515–26520, Nov. 2016.
- [15] G. Sobon, J. Sotor, A. Przewolka, I. Pasternak, W. Strupinski, and K. Abramski, "Amplification of noise-like pulses generated from a graphene-based Tm-doped all-fiber laser," *Opt. Exp.*, vol. 24, no. 18, pp. 20359–20364, Sep. 2016.
- [16] Q. Wang, T. Chen, B. Zhang, A. P. Heberle, and K. P. Chen, "All-fiber passively mode-locked thulium-doped fiber ring oscillator operated at solitary and noiselike modes," *Opt. Lett.*, vol. 36, no. 19, pp. 3750–3752, Oct. 2011.
- [17] X. He *et al.*, "60 nm bandwidth, 17 Nj noiselike pulse generation from a thulium-doped fiber ring laser," *Appl. Phys. Exp.*, vol. 6, no. 11, Nov. 2013, Art. no. 112702.
- [18] J. Li *et al.*, "Thulium-doped all-fiber mode-locked laser based on Npr and 45 degrees-tilted fiber grating," *Opt. Exp.*, vol. 22, no. 25, pp. 31020–31028, Dec. 2014.
- [19] G. Sobon, J. Sotor, T. Martynkien, and K. M. Abramski, "Ultra-broadband dissipative soliton and noise-like pulse generation from a normal dispersion mode-locked Tm-doped all-fiber laser," *Opt. Exp.*, vol. 24, no. 6, pp. 6156–6161, Mar. 2016.
- [20] J. Li *et al.*, "All-fiber passively mode-locked Tm-doped NOLM-based oscillator operating at 2- $\mu$ m in both soliton and noisy-pulse regimes," *Opt. Exp.*, vol. 22, no. 7, pp. 7875–7882, Apr. 2014.
- [21] S. Liu, F.-P. Yan, L.-N. Zhang, W.-G. Han, Z.-Y. Bai, and H. Zhou, "Noise-like femtosecond pulse in passively mode-locked Tm-doped NALM-based oscillator with small net anomalous dispersion," *J. Opt.*, vol. 18, no. 1, Jan. 2016, Art. no. 015508.
- [22] M. Michalska and J. Swiderski, "Noise-like pulse generation using polarization maintaining mode-locked thulium-doped fiber laser with nonlinear amplifying loop mirror," *IEEE Photon. J.*, vol. 11, no. 6, Dec. 2019, Art. no. 1504710.
- [23] M. Wang *et al.*, "10  $\mu$ j noise-like pulse generated from all fiberized Tm-doped fiber oscillator and amplifier," *Opt. Exp.*, vol. 29, no. 7, pp. 10172–10180, Mar. 2021.
- [24] K. Zhao *et al.*, "High-energy dissipative soliton resonance and rectangular noise-like pulse in a figure-9 Tm fiber laser," *Appl. Phys. Exp.*, vol. 12, no. 1, Jan. 2019, Art. no. 012002.
- [25] S. Liu *et al.*, "Single-polarization noise-like pulse generation from a hybrid mode-locked thulium-doped fiber laser," *J. Opt.*, vol. 19, no. 4, Apr. 2017, Art. no. 045505.
- [26] J. Sotor *et al.*, "All-polarization-maintaining, stretched-pulse Tm-doped fiber laser, mode-locked by a graphene saturable absorber," *Opt. Lett.*, vol. 42, no. 8, pp. 1592–1595, Apr. 2017.
- [27] L. M. Zhao and D. Y. Tang, "Generation of 15-Nj bunched noise-like pulses with 93-Nm bandwidth in an erbium-doped fiber ring laser," *Appl. Phys. B*, vol. 83, no. 4, pp. 553–557, 2006.
- [28] G. Sobon, J. Sotor, T. Martynkien, and K. M. Abramski, "Ultra-broadband dissipative soliton and noise-like pulse generation from a normal dispersion mode-locked Tm-doped all-fiber laser," *Opt. Exp.*, vol. 24, no. 6, pp. 6156–6161, Mar. 2016.